

# Docking Study, Synthesis, Characterization and Preliminary Cytotoxic Evaluation of new 1,2,3,4-Tetrahydropyrimidine Derivatives

Noor M. Mohammed\*

Department of Pharmaceutical Chemistry, College of Pharmacy, University of Baghdad, Baghdad, Iraq.

\*Correspondence to: Noor M. Mohammed (E-mail: non.myo.86@gmail.com)

(Submitted: 03 September 2022 – Revised version received: 12 September 2022 – Accepted: 27 September 2022 – Published Online: 26 October 2022)

## Abstract

**Objective:** This study resolved that these anew synthesized analogs may be embodied as an exploitable foundation of new anticancer agents to competition breast cancer.

**Methods:** By means of the crystal structure of Histone deacetylases (HDACs-8) with Vorinostat (SAHA) as a co-crystalized ligand was gained from the protein data-bank (PDB code 4QA0) as a result of docking the compounds (V a,s, V b,s, V a,t and V b,t) give good docking scores compared to the standard. Compounds (V a,s, V b,s, V a,t and V b,t) was synthesized by multistep procedures from the reaction of intermediate derivatives (IV a,b) and the thiosemicarbazide or semicarbazide. The chemical structures of the target compounds and their intermediates were confirmed by FT-IR and <sup>1</sup>H NMR.

**Results:** The *in-vitro* cytotoxicity assay (MTT assay) demonstrated that compounds V a,t and V b,t showed good inhibition ratios in Breast cancer cell line (MCF-7) and human colon adenocarcinoma (HRT-18) comparable with drug control Vorinostat (SAHA).

**Conclusion:** From the docking study, it was concluded that C=S moiety were very successful to bind tightly to the zinc binding group of HDAC enzyme by making numerous interaction modes.

**Keywords:** Anticancer, MCF-7, HRT-18, semicarbazide, Dihydropyrimidine, thiosemicarbazide, docking study

## Introduction

Epigenetic changes in cancer are common and associated with pathogenesis and molecular heterogeneity.<sup>1</sup> Carcinogenesis results from the interplay between the activation of oncogenes and the inactivation of tumor suppressor genes. One of the causes of the latter is switching off the gene in concern by epigenetic changes rather than by mutation of the DNA sequence. These reversible epigenetic changes do not involve alteration of the nucleotide sequence of DNA but, instead, are due to inappropriate DNA methylation, chromatin remodeling, and changes in small noncoding RNAs.<sup>2</sup>

Epigenetic machineries that alter chromatin structure can be divided into four main classes: DNA methylation, covalent histone modifications, non-covalent mechanisms such as incorporating histone variants, and nucleosome remodelling and non-coding RNAs, including miRNAs.<sup>3</sup> These alterations work collected to control the operative of the genome by altering the local structural dynamics of chromatin, primarily controlling its convenience and compactness. The interplay of these modifications creates an 'epigenetic landscape' that regulates the way the mammalian genome manifests itself in different cell types, developmental stages, and disease states, including cancer.<sup>4</sup>

Histone deacetylases (HDACs) have received significant attention in the research area of epigenetics. Acetylation by HATs transfers an acetyl group and neutralizes the positive charge of lysine residues in the histone tail resulting in loosening histone-DNA interactions and allowing access of transcription factors to DNA. The stimulatory effect of HATs on gene expression is reversed by HDACs, which remove an acetyl group from the terminal amino group of a lysine residue, leaving a positive charge, that tightly interacts with the negative amount of DN, promotes chromatin condensation, and thereby repress transcription and induce gene silencing.

Thereby, HATs are co-activators, and the HDACs are co-repressors.<sup>5</sup>

Any imbalance between the activities of these two opposite enzyme families would disturb the normal histone acetylation homeostasis. Overexpression of HDACs, i.e., hypoacetylation, is involved in cancer generation and cancer progress since tumor suppressor gene transcription is prevented due to the inactivated chromatin system. There would be alteration in proliferation, differentiation, and apoptosis fashion of normal cells becoming malignant. Hypoacetylation is also involved in the loss of cell adhesion, migration, invasion, and angiogenesis, resulting in cancer start and progress.<sup>6</sup>

HDACs are overexpressed in several types of cancer cells compared to normal cells. For example, breast cancer cells show measurable levels of HDACs 1, 2, and 3, while normal breast cells do not show any.<sup>7,8</sup> This finding could be of great clinical value for targeting these enzymes in breast cancer. Besides, the specificity of HDACs against the other types of cancer cells is still of great importance; the importance of inhibition of elevated levels of these enzymes in cancer cells outweighs inhibition of low levels in normal cells. Furthermore, the relative specificity of HDACs between cancer cells and normal cells may be attributed to the idea hypothesized that, in contrast to cancer cells, normal cells could withstand the inhibitory action of HDACs and compensate for the inhibited vital pathways since they have multiple, alternative epigenetic regulatory ways.<sup>9</sup>

Histone deacetylase inhibitors (HDACIs) have emerged as a novel session of anti-cancer agents that show essential parts in epigenetic rule of gene expression, making death, apoptosis, and cell cycle arrest in cancer cells. Several HDACIs with much more potent anticancer effects and diverse structures have been identified; they include natural or synthetic products.<sup>10</sup> Recently, many HDAC inhibitors

have been clinically validated in cancer patients resulting in the approval of five HDACi, vorinostat, romidepsin, belinostat and panobinostat by the FDA and chidamide by Chinese FDA for the treatment of cutaneous, peripheral T-cell lymphoma (CTCL, PTCL) multiple myeloma (MM) and acute myeloid leukemia (AML).<sup>11,12</sup> SAHA, belinostat, and panobinostat are pan-HDACi since they targeting multiple HDAC isoforms, while romidepsin is a selective one.<sup>13,14</sup> Several new HDACi are in different stages of clinical development for the treatment of haematological malignancies as well as solid tumours. HDACi have the potential to be used as monotherapies or in combination with other anticancer therapies.<sup>15</sup> Also, great efforts are exerted to discover novel HDACi for use as anti-cancer drugs alone or in combination and have isoform selectivity are continuing by researchers.<sup>16</sup>

The "classical" HDAC-Is act exclusively on HDAC Classes I, II and IV by binding to the zinc-enriched catalytic domain of the HDACs. Figure 1 show the main four classes of HDAC inhibitors and the FDA-approved ones. Classical HDAC-Is are subdivided according to the chemical moiety that binds to the zinc ion (except cyclic tetrapeptides which bind to the zinc ion with a thiol group). Some examples in decreasing order of the typical zinc binding affinity:<sup>17</sup>

1. Hydroxamic acids (orhydroxamates) the major group, such as Vorinostat (SAHA), Belinostat and Panobinostat
2. Cyclic tetrapeptides such as Romidepsin or Depsipeptides,
3. Benzamides or o-aminoanilides, Mocetinostat, Chidamide and Etinostat
4. The aliphatic acid such as Phenylbutyrate and Valproic acid.

## Materials and Methods

### Materials

4-chlorobenzaldehyde, Benzaldehyde was purchased from Hyper Chem China. Other chemicals were purchased from Sigma-Aldrich. All chemicals are of analytical grade, and they were used as received without further purification.

### Characterization of Compounds (V a,s, V b,s, Va,t and V b,t)

Melting points, Fourier transform infrared spectroscopy: FTIR, NMR: H-NMR spectra, were performed for compound characterization.

### Molecular Docking

Vorinostat (SAHA) was used to validate the docking process because the PDB obtained has a crystal structure of the protein and bound Vorinostat (SAHA).

### Histone Deacetylase Enzyme<sup>18,19</sup>

The Molecular Operating Environment (MOE) software version 2015.10 was used to conduct the docking studies (Chemical Computing Group, Montreal, Canada). HDAC-8 (PDB code 4QA0) X-ray crystal structures were retrieved from the Protein Data Base (PDB).

All water molecules were removed from PDB files, and hydrogen atoms were then added to the protein. The MOE-Dock algorithm was then used to dock the optimized shape of the chemical into the binding site.

The London dG was selected as the initial scoring method and the Rigid Receptor was selected as the final scoring method. The best 5 poses of each ligand were retained and scored. Finally, the geometry of docked complex was analyzed by the pose viewer utility in MOE.

### Chemical Synthesis

#### Synthesis of Dihydropyrimidine Derivatives (I a,b)

A mixture of aldehydes (10 mmol), Ethyl acetoacetate (10 mmol), urea (15 mmol) and 10 ml of ethanol and (4 mmol) of Ammonium chloride, was refluxed for 7-8 hours. Then the reaction mixture was neutralized with 1N HCl. The precipitate was filtered and recrystallized from ethanol.<sup>20</sup>

Title ethyl 6-methyl-2-oxo-4-phenyl-1,2,3,4-tetrahydropyrimidine-5-carboxylate (I a) was obtained as a pale off-white powder, mp. 204–207°C, yield 88%. The FT-IR for I a, 2978 cm<sup>-1</sup> C-H Asymmetric str. Vibration of aliphatic CH<sub>2</sub>, 1697 cm<sup>-1</sup> Carbonyl str. vibration band of ester, 1643 cm<sup>-1</sup>

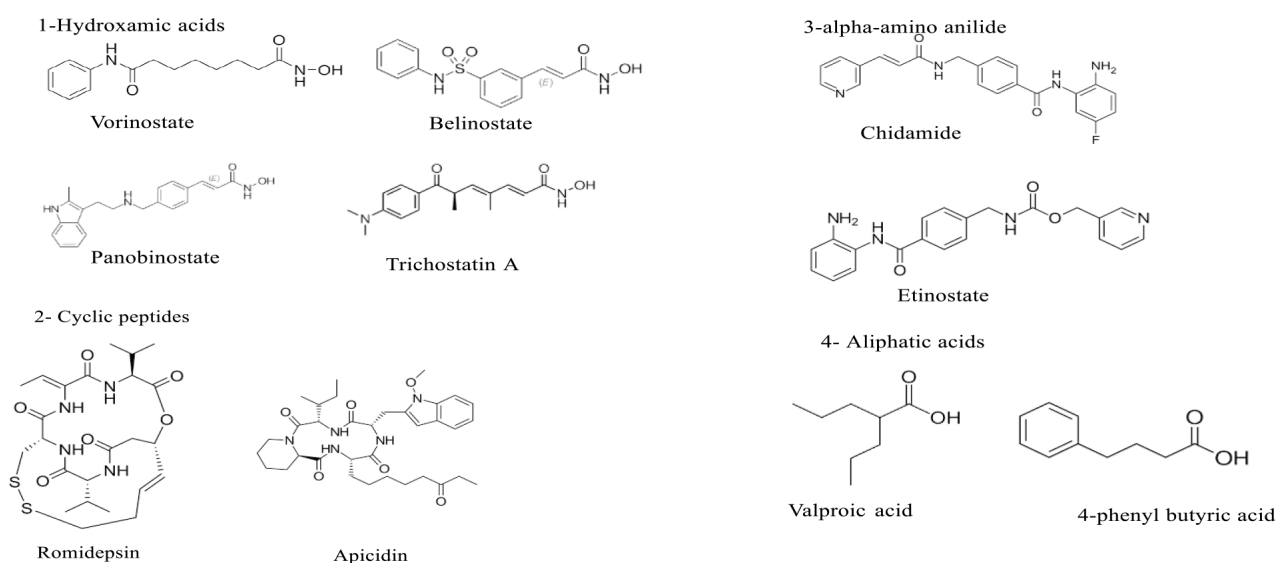
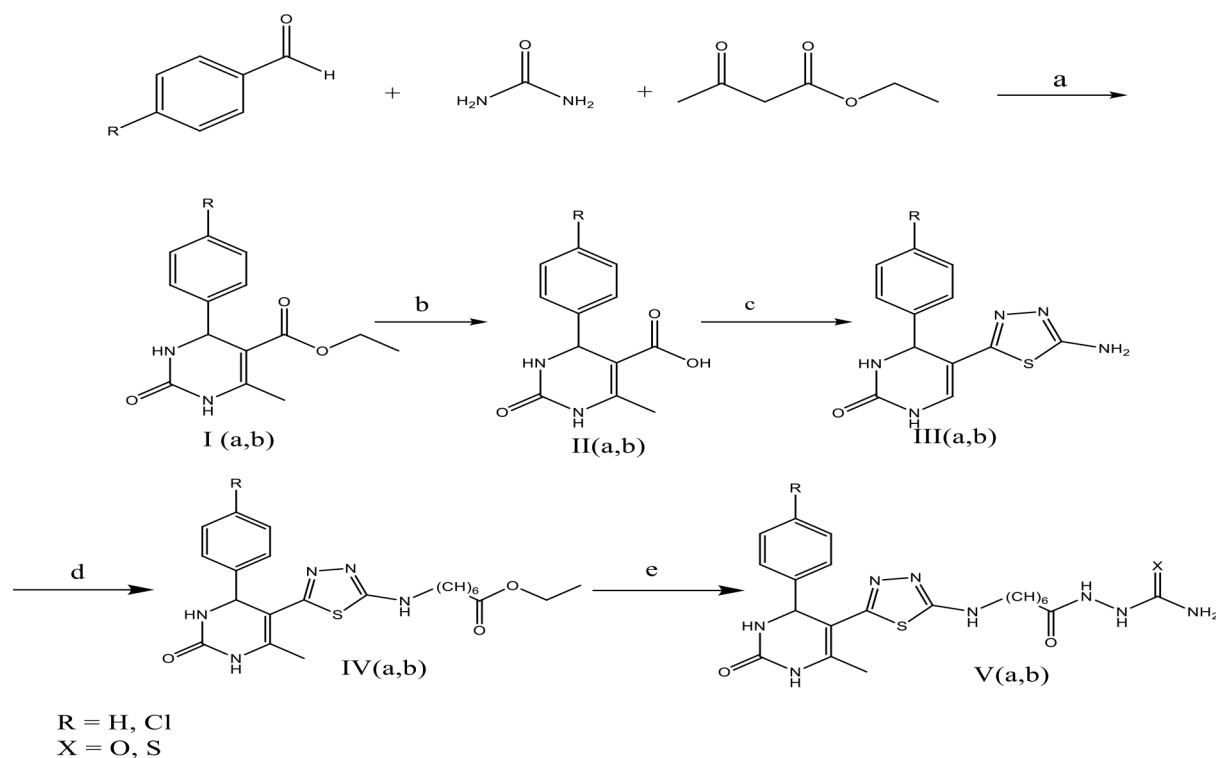


Fig. 1 The main four classes of HDAC inhibitors.



Scheme 1. **Synthesis schematics of compound (V a,s – V b,t). Reagents and conditions: (a) Reflux 7-8 hr. abs. ethanol (b) Hydrolysis by 15% NaOH (c) Thiosemicarbazide, 70% sulfuric acid in ethanol, ammonia (d) Ethyl-7-bromoheptanoate, dry K<sub>2</sub>CO<sub>3</sub> in anhydrous acetone (e) Thiosemicarbazide, semicarbazide, methanol, KOH.**

Carbonyl str. vibration band of amide, 1311  $\text{cm}^{-1}$  C-N str. Vibration of amide, 1215  $\text{cm}^{-1}$  C-O str. Vibration of ester. <sup>1</sup>H NMR (400 MHz, DMSO-d<sub>6</sub>)  $\delta$  1.123-1.152 (t, J = 5.0 Hz, 3H), 4.159-4.202 (q, J = 4.1 Hz, 3H), 2.3141 (s, J = 7.2 Hz, 3H), 5.424-5.439 (d, J = 5.0 Hz, 1H), 7.298-7.318 (m, 5H). And ethyl 4-(4-chlorophenyl)-6-methyl-2-oxo-1,2,3,4-tetrahydropyrimidine-5-carboxylate compound (I b) was obtained as a pale-yellow powder mp. 214-216°C, yield 82%. The FT-IR for I b, 2954  $\text{cm}^{-1}$  C-H Asymmetric str. Vibration of aliphatic CH<sub>2</sub> 1701  $\text{cm}^{-1}$  Carbonyl str. vibration band of ester, 1647  $\text{cm}^{-1}$  Carbonyl str. vibration band of amide, 1323  $\text{cm}^{-1}$  C-N str. Vibration of amide, 1219  $\text{cm}^{-1}$  C-O str. Vibration of ester. <sup>1</sup>H NMR (400 MHz, DMSO-d<sub>6</sub>)  $\delta$  1.123-1.152 (t, J = 5.0 Hz, 3H), 4.159-4.202 (q, J = 4.1 Hz, 3H), 2.3121 (s, J = 7.2 Hz, 3H), 5.411 (d, J = 5.0 Hz, 1H), 7.292-7.306 (m, 2H).

### Ester Hydrolysis (II a,b)

A stirring mixture of compounds (I a, b) (10 mmol) and sodium hydroxide (15%, 10 ml) was refluxed for 12-15 hours at 90°C. After cooling, the solution was acidified with (1N) hydrochloric acid and the precipitate was filtered and recrystallized from ethanol.<sup>21</sup>

The title 6-methyl-2-oxo-4-phenyl-1,2,3,4-tetrahydropyrimidine-5-carboxylic acid (II a) was obtained as a pale-yellow powder, mp. 221-223°C, yield 76%. The FT-IR for II a, 3400-2800  $\text{cm}^{-1}$  O-H Vibration of carboxylic acid, 3028  $\text{cm}^{-1}$  C-H Asymmetric str. Vibration of an aromatic ring, 1693  $\text{cm}^{-1}$  Carbonyl str. vibration band of carboxylic acid, 1597  $\text{cm}^{-1}$  Carbonyl str. vibration band of amide, 1311  $\text{cm}^{-1}$  C-N str. Vibration of amide. <sup>1</sup>H NMR (400 MHz, DMSO-d<sub>6</sub>)  $\delta$  12.36 (s, 1H), 9.90 (d, 1H), 7.35-7.27 (m, 6H), 5.35 (d, J = 7.5 Hz, 1H), 2.23 (s, 3H). And 4-(4-chlorophenyl)-6-methyl-2-oxo-1,2,3,4-tetrahydropyrimidine-5-carboxylic

acid compound (II b) was obtained as a white powder mp. 227-229°C, yield 72%. The FT-IR for II b, 3400-2800  $\text{cm}^{-1}$  O-H Vibration of carboxylic acid, 3093  $\text{cm}^{-1}$  C-H Asymmetric str. Vibration of an aromatic ring, 1697  $\text{cm}^{-1}$  Carbonyl str. vibration band of carboxylic acid, 1674  $\text{cm}^{-1}$  Carbonyl str. vibration band of amide, 1284  $\text{cm}^{-1}$  C-N str. Vibration of amide, 817  $\text{cm}^{-1}$  C-Cl str. Vibration. <sup>1</sup>H NMR (400 MHz, DMSO-d<sub>6</sub>) 12.36 (s, 1H), 9.90 (s, 1H), 7.39 (d, J = 8.3 Hz, 2H), 7.33-7.28 (m, 3H), 5.34 (d, J = 7.7 Hz, 1H), 2.23 (s, 3H).

### Synthesis of 1,3,4-Thiadiazole-2-Amino Derivatives Synthesis (III a,b)

A mixture of thiosemicarbazide (5 mmol), compounds (II a,b) (5 mmol) and 70% sulfuric acid in ethanol. Was cool and stirred overnight and then refluxed at a temperature of 80-90°C for 7 hours. The reaction mixture was cool and neutralized with concentrated ammonia checked by litmus paper to PH 4. The precipitate was filtered and recrystallized from ethanol.<sup>22</sup>

The title 5-(5-amino-1,3,4-thiadiazol-2-yl)-6-methyl-4-phenyl-3,4-dihydropyrimidin-2(1H)-one compound (III a) was obtained as a white powder, mp. 170-172°C, yield 78%. The FT-IR for III a, 3348  $\text{cm}^{-1}$  N-H str. Vibration of amide, 3286, 3202  $\text{cm}^{-1}$  N-H str. Vibration of primary amine, 3066  $\text{cm}^{-1}$  C-H Asymmetric str. Vibration of aromatic ring, 1500  $\text{cm}^{-1}$  C=C str. Vibration of aromatic ring, 1315  $\text{cm}^{-1}$  C-N str. Vibration of amide, 694  $\text{cm}^{-1}$  C-S-C str. vibration band. <sup>1</sup>H NMR (400 MHz, DMSO-d<sub>6</sub>)  $\delta$  10.02 (s, 1H), 8.14 (d, J = 7.3 Hz, 1H), 7.45 (d, J = 8.5 Hz, 1H), 7.38 (t, J = 7.6 Hz, 2H), 7.31 (d, J = 7.5 Hz, 1H), 7.02 (s, 2H), 5.67 (d, J = 6.9 Hz, 1H), 2.19 (s, 3H). The title 5-(5-amino-1,3,4-thiadiazol-2-yl)-4-(4-chlorophenyl)-6-methyl-3,4-dihydropyrimidin-2(1H)-one compound (III b) was obtained as a pale off white powder, mp.

174–176°C, yield 81%. The FT-IR for III b, 33483352  $\text{cm}^{-1}$  N-H str. Vibration of amide, 3201  $\text{cm}^{-1}$  NH str. Vibration of primary amine, 3051  $\text{cm}^{-1}$  C-H Asymmetric str. Vibration of aromatic ring, 1566  $\text{cm}^{-1}$  C=C str. Vibration of aromatic ring, 1311  $\text{cm}^{-1}$  C-N str. Vibration of amide, 813  $\text{cm}^{-1}$  C-Cl str. Vibration, 702  $\text{cm}^{-1}$  C-S-C str. vibration band.  $^1\text{H}$  NMR (400 MHz, DMSO-d<sub>6</sub>)  $\delta$  1H NMR (500 MHz, DMSO-d<sub>6</sub>)  $\delta$  10.02 (s, 1H), 8.14 (d, J = 7.3 Hz, 1H), 7.34 (d, J = 8.1 Hz, 2H), 7.30 (d, J = 8.1 Hz, 2H), 7.02 (s, 2H), 5.70 (d, J = 7.5 Hz, 1H), 2.19 (s, 3H).

### Amine alkylation (IV a,b)

A mixture of compound (III a,b) (7.9 mmol), ethyl-7-bromoheptanoate (7.9 mmol) and dry K<sub>2</sub>CO<sub>3</sub> (23.8 mmol) in anhydrous acetone (20 mL) was stirred under reflux. After 24 hours at 70°C. Upon completion of the reaction (as indicated by TLC), the solvent was reduced. The resulted precipitate was filtered and washed with distilled water and recrystallized from ethanol.<sup>23</sup>

The title ethyl 7-((5-(6-methyl-2-oxo-4-phenyl-1,2,3,4-tetrahydropyrimidin-5-yl)-1,3,4-thiadiazol-2-yl) amino) heptanoate compound (IV a) was obtained as a pale-yellow powder mp. 200–203°C, yield 88%. The FT-IR for IV a, 3309  $\text{cm}^{-1}$  N-H str. Vibration of amide, 2939  $\text{cm}^{-1}$  C-H Asymmetric str. Vibration of aliphatic CH<sub>3</sub>, 1732  $\text{cm}^{-1}$  Carbonyl str. vibration band of ester, 1651  $\text{cm}^{-1}$  Carbonyl str. vibration band of amide, 1597  $\text{cm}^{-1}$  C=N str. Vibration, 1535  $\text{cm}^{-1}$  C=C Symmetric str. Vibration of aromatic ring, 1454  $\text{cm}^{-1}$  C-H asymmetric and symmetric str. Vibration of (CH<sub>2</sub>)<sub>6</sub>, 1377  $\text{cm}^{-1}$  C-H asymmetric and symmetric str. Vibration of (CH<sub>2</sub>-CH<sub>3</sub>), 1311  $\text{cm}^{-1}$  C-N str. Vibration of amide, 1203  $\text{cm}^{-1}$  O-C str. Vibration, 686  $\text{cm}^{-1}$  C-S-C str. Vibration.  $^1\text{H}$  NMR (400 MHz, DMSO-d<sub>6</sub>)  $\delta$  9.97 (s, 1H), 8.14 (d, J = 7.3 Hz, 1H), 7.50 (t, J = 4.7 Hz, 1H), 7.45 (d, J = 8.5 Hz, 2H), 7.38 (t, J = 7.6 Hz, 2H), 7.31 (d, J = 7.5 Hz, 1H), 5.67 (d, J = 7.3 Hz, 1H), 4.10 (q, J = 6.5 Hz, 2H), 3.47 (q, 2H), 2.29 (t, J = 8.5 Hz, 2H), 2.19 (s, 3H), 1.67 – 1.49 (m, 4H), 1.40–1.23 (m, 4H), 1.16 (t, J = 6.7 Hz, 3H). And ethyl 7-((5-(4-(4-chlorophenyl)-6-methyl-2-oxo-1,2,3,4-tetrahydropyrimidin-5-yl)-1,3,4-thiadiazol-2-yl) amino) heptanoate compound (IV b) was obtained as off-white powder mp. 204–206°C, yield 76%. The FT-IR for IV b, 3414  $\text{cm}^{-1}$  N-H str. Vibration of amide, 2981  $\text{cm}^{-1}$  C-H Asymmetric str. Vibration of aliphatic CH<sub>3</sub>, 1732  $\text{cm}^{-1}$  Carbonyl str. vibration band of ester, 1678  $\text{cm}^{-1}$  Carbonyl str. vibration band of amide, 1604  $\text{cm}^{-1}$  C=N str. Vibration, 1573  $\text{cm}^{-1}$  C=C Symmetric str. Vibration of aromatic ring, 1462  $\text{cm}^{-1}$  C-H asymmetric and symmetric str. Vibration of (CH<sub>2</sub>)<sub>6</sub>, 1377  $\text{cm}^{-1}$  C-H asymmetric and symmetric str. Vibration of (CH<sub>2</sub>-CH<sub>3</sub>), 1315  $\text{cm}^{-1}$  C-N str. Vibration of amide, 1199  $\text{cm}^{-1}$  O-C str. Vibration, 813  $\text{cm}^{-1}$  C-Cl str. Vibration, 698  $\text{cm}^{-1}$  C-S-C str. Vibration.  $^1\text{H}$  NMR (400 MHz, DMSO-d<sub>6</sub>)  $\delta$  9.97 (s, 1H), 8.14 (d, J = 7.4 Hz, 1H), 7.50 (t, J = 4.7 Hz, 1H), 7.34 (d, J = 8.2 Hz, 2H), 7.30 (d, J = 8.2 Hz, 2H), 5.70 (d, J = 6.8 Hz, 1H), 4.10 (q, J = 6.6 Hz, 2H), 3.47 (q, 2H), 2.29 (t, J = 8.5 Hz, 2H), 2.19 (s, 3H), 1.67–1.49 (m, 4H), 1.40–1.24 (m, 4H), 1.16 (t, J = 6.6 Hz, 3H).

### Synthesis of Amid (V a,s – V b,t)

To a solution of thiosemicarbazide or semicarbazide (34.8 mmol) in 10 mL methanol, KOH (34.8 mmol) was added. The reaction mixture was stirred for 10 min at 40°C, and was then cooled to 0°C and filtered. Compound (IV a,b) (320 mg, 1.1 mmol) was added to the filtrate, after which the reaction was

stirred at room temperature for 30 min. The solvent was removed under reduced pressure, diluted with a saturated Ammonium chloride aqueous solution, and extracted with ethyl acetate. The organic layer was dried over Sodium sulfate. The resulting solution was evaporated under reduced pressure.<sup>24</sup>

The title 2-(7-((5-(6-methyl-2-oxo-4-phenyl-1,2,3,4-tetrahydropyrimidin-5-yl)-1,3,4-thiadiazol-2-yl) amino) heptanoyl) hydrazine-1-carboxamide Compound (V a,s) was obtained as a white powder mp. 269–271°C, yield 83%. The FT-IR for V a,s, 3421  $\text{cm}^{-1}$  N-H str. Vibration of secondary amide, 3353,3267  $\text{cm}^{-1}$  N-H str. Vibration of primary amide 2985  $\text{cm}^{-1}$  C-H Asymmetric str. Vibration of aliphatic CH<sub>3</sub>, 1693  $\text{cm}^{-1}$  Carbonyl str. vibration band of dihydropyrimidin ring, 1647  $\text{cm}^{-1}$  Carbonyl str. vibration band of amide (CH<sub>2</sub>)<sub>6</sub>, 1600  $\text{cm}^{-1}$  Carbonyl str. vibration band of primary amide, 1573  $\text{cm}^{-1}$  C=N str. Vibration, 1531  $\text{cm}^{-1}$  C=C Symmetric str. Vibration of aromatic ring, 1454  $\text{cm}^{-1}$  C-H asymmetric and symmetric str. Vibration of (CH<sub>2</sub>)<sub>6</sub>, 1288  $\text{cm}^{-1}$  C-N str. Vibration of amide, 698  $\text{cm}^{-1}$  C-S-C str. Vibration.  $^1\text{H}$  NMR (400 MHz, DMSO-d<sub>6</sub>)  $\delta$  9.97 (s, 1H), 9.62 (d, J = 6.3 Hz, 1H), 8.95 (d, J = 6.3 Hz, 1H), 8.14 (d, J = 7.4 Hz, 1H), 7.50 (t, J = 4.7 Hz, 1H), 7.44 (d, J = 6.2 Hz, 2H), 7.38 (t, J = 7.6 Hz, 2H), 7.31 (d, J = 7.4 Hz, 1H), 6.44 (s, 2H), 5.68 (d, J = 8.2 Hz, 1H), 3.46 (q, 2H), 2.24 – 2.17 (m, 5H), 1.67 – 1.51 (m, 4H), 1.40 – 1.27 (m, 4H). The title 2-(7-((5-(4-(4-chlorophenyl)-6-methyl-2-oxo-1,2,3,4-tetrahydropyrimidin-5-yl)-1,3,4-thiadiazol-2-yl) amino) heptanoyl) hydrazine-1-carboxamide compound (V b,s) was obtained as a pale yellow powder mp. 273–275°C, yield 87%. The FT-IR for V b,s, 3464  $\text{cm}^{-1}$  N-H str. Vibration of secondary amide, 3066,3035  $\text{cm}^{-1}$  N-H str. Vibration of primary amide 2985  $\text{cm}^{-1}$  C-H Asymmetric str. Vibration of aliphatic CH<sub>3</sub>, 1708  $\text{cm}^{-1}$  Carbonyl str. vibration band of dihydropyrimidin ring, 1670  $\text{cm}^{-1}$  Carbonyl str. vibration band of amide (CH<sub>2</sub>)<sub>6</sub>, 1604  $\text{cm}^{-1}$  Carbonyl str. vibration band of primary amide, 1577  $\text{cm}^{-1}$  C=N str. Vibration, 1531  $\text{cm}^{-1}$  C=C Symmetric str. Vibration of aromatic ring, 1465  $\text{cm}^{-1}$  C-H asymmetric and symmetric str. Vibration of (CH<sub>2</sub>)<sub>6</sub>, 1288  $\text{cm}^{-1}$  C-N str. Vibration of amide, 825  $\text{cm}^{-1}$  C-Cl str. Vibration, 698  $\text{cm}^{-1}$  C-S-C str. Vibration. The  $^1\text{H}$  NMR (400 MHz, DMSO-d<sub>6</sub>)  $\delta$  9.97 (s, 1H), 9.62 (d, J = 6.4 Hz, 1H), 8.95 (d, J = 6.4 Hz, 1H), 8.14 (d, J = 7.3 Hz, 1H), 7.50 (t, J = 4.6 Hz, 1H), 7.34 (d, J = 8.0 Hz, 2H), 7.30 (d, J = 8.3 Hz, 2H), 6.44 (s, 2H), 5.70 (d, J = 7.8 Hz, 1H), 3.47 (q, 2H), 2.24 – 2.17 (m, 5H), 1.67–1.51 (m, 4H), 1.40–1.28 (m, 4H). The title 2-(7-((5-(6-methyl-2-oxo-4-phenyl-1,2,3,4-tetrahydropyrimidin-5-yl)-1,3,4-thiadiazol-2-yl) amino) heptanoyl) hydrazine-1-carbothioamide compound (V a,t) was obtained as a white powder mp. 191–193°C, yield 89%. The FT-IR for V a,t, 3394  $\text{cm}^{-1}$  N-H str. Vibration of secondary amide, 3240, 3151  $\text{cm}^{-1}$  N-H str. Vibration of primary amide 2985  $\text{cm}^{-1}$  C-H Asymmetric str. Vibration of aliphatic CH<sub>3</sub>, 1697  $\text{cm}^{-1}$  Carbonyl str. vibration band of dihydropyrimidin ring, 1651  $\text{cm}^{-1}$  Carbonyl str. vibration band of amide (CH<sub>2</sub>)<sub>6</sub>, 1597  $\text{cm}^{-1}$  C=N str. Vibration, 1527  $\text{cm}^{-1}$  C=C Symmetric str. Vibration of aromatic ring, 1454  $\text{cm}^{-1}$  C-H asymmetric and symmetric str. Vibration of (CH<sub>2</sub>)<sub>6</sub>, 1288  $\text{cm}^{-1}$  C-N str. Vibration of amide, 1261  $\text{cm}^{-1}$  C=S str. Vibration, 698  $\text{cm}^{-1}$  C-S-C str. Vibration.  $^1\text{H}$  NMR (400 MHz, DMSO-d<sub>6</sub>)  $\delta$  10.05 (d, J = 5.4 Hz, 1H), 9.97 (s, 1H), 9.08 (d, J = 5.1 Hz, 1H), 8.14 (d, J = 7.3 Hz, 1H), 7.50 (t, J = 4.6 Hz, 1H), 7.44 (d, J = 5.8 Hz, 2H), 7.38 (t, J = 7.7 Hz, 2H), 7.31 (d, J = 7.4 Hz, 1H), 7.28 (s, 2H), 5.67 (d, J = 7.7 Hz,

1H), 3.47 (q, 2H), 2.24–2.17 (m, 5H), 1.67–1.51 (m, 4H), 1.40–1.27 (m, 4H). the title 2-(7-((5-(4-(4-chlorophenyl)-6-methyl-2-oxo-1,2,3,4-tetrahydropyrimidin-5-yl)-1,3,4-thiadiazol-2-yl) amino) heptanoyl) hydrazine-1-carbothioamide compound (V b,t) was obtained as a pale off white powder mp. 196–19°C, yield 82%. The FT-IR for V b,t, 3221  $\text{cm}^{-1}$  N-H str. Vibration of secondary amide, 3066, 3035  $\text{cm}^{-1}$  N-H str. Vibration of primary amide 2985  $\text{cm}^{-1}$  C-H Asymmetric str. Vibration of aliphatic CH<sub>3</sub>, 1689  $\text{cm}^{-1}$  Carbonyl str. vibration band of amide (CH<sub>2</sub>)<sub>6</sub>, 1600  $\text{cm}^{-1}$  C=N str. Vibration, 1531  $\text{cm}^{-1}$  C=C Symmetric str. Vibration of aromatic ring, 1462  $\text{cm}^{-1}$  C-H asymmetric and symmetric str. Vibration of (CH<sub>2</sub>)<sub>6</sub>, 1288  $\text{cm}^{-1}$  C-N str. Vibration of amide, 1261  $\text{cm}^{-1}$  C=S str. Vibration, 8117  $\text{cm}^{-1}$  C-Cl str. Vibration, 686  $\text{cm}^{-1}$  C-S-C str. Vibration.

<sup>1</sup>H NMR (400 MHz, DMSO-d<sub>6</sub>)  $\delta$ 10.05 (d, J = 5.4 Hz, 1H), 9.97 (s, 1H), 9.08 (d, J = 5.1 Hz, 1H), 8.14 (d, J = 7.3 Hz, 1H), 7.50 (t, J = 4.6 Hz, 1H), 7.34 (d, J = 8.0 Hz, 2H), 7.32 – 7.26 (m, 4H), 5.70 (d, J = 8.9 Hz, 1H), 3.47 (q, 2H), 2.24 – 2.17 (m, 5H), 1.67 – 1.51 (m, 4H), 1.40 – 1.28 (m, 4H).

### In Vitro Cytotoxicity Assay<sup>25,26</sup>

The *in vitro* cytotoxicity of compounds V a,s, V b,s, V a,t, and V b,t were evaluated by MTT assay on human breast cancer cells (MCF-7) and human colon adenocarcinoma (HRT-18). MTT was performed to determine the cytotoxic effect of the samples at various concentrations. The results were given as the mean of three independent experiments and the IC<sub>50</sub> values were then calculated.

### Statistical Analysis

The results of the experimental work were demonstrated as the standard error of the mean (SEM) for triplicate data by using nonlinear regression analysis (Prism Pad 8.1).

## Results

### Molecular Docking

#### Binding site of SAHA

The binding site of HDAC-8 is formed like a cleft which contains a deep pocket that mainly made up of Phe152, Met274, Gly152, His142, His143, Trp142, Gly304, Tyr306, Asp187, Asp267, Asp101, His180 and Phe208. The deep pocket prefers non hydrophobic moieties such as NH and C=S fragments.

According to the result of docking as shown in Table 1 and Figures 2–6, V a,s, V b,s, V a,t, and V b,t give very good docking scores compared to the standard (SAHA) since synthetic compounds interacted with the most residues in the active site (predominantly hydrogen bond).

The V a,t appear to has more binding tendency with HDAC-8 via zinc binding group (C=S) spacer and also thiadiazol ring (good fitting) (His142, His143 and Zn401) while V a,s which bind through zinc binding group (C=O), The C=S group of the V b,t aid to more binding tendency (good fitting) (Tyr306 and Zn401) due to the effect of zinc binding group than C=O of V b,s.

### Synthesis of Compounds (I a,b – Va,t, b,t)

Compound (I a,b) was synthesized by the reaction of aldehydes, Ethyl acetoacetate, urea and Ammonium chloride in the presence of ethanol. The FTIR for both compounds were characterized by disappearance of C=O band of aldehyde in

Table 1. The results of interactions of the ligands with HDAC-8

Compound ID	Docking score (kcal/mol)	H-bond interaction	Coordinating bond length (with zinc) [Å]
SAHA	-8.69	Tyr306(2.98)	2.17
V a,s	-9.21	Gly151(3.19), Asp178(3.56), Tyr306(3.13)	1.99
V b,s	-10.25	Gly151(3.12), His143(3.07)	1.98
V a,t	-8.25	Gly151(2.98), His142(3.16), His143(3.19), Tyr306(2.94)	2.18
V b,t	-8.63	Gly151(2.82), Tyr306(3.20), His143(3.06)	2.17

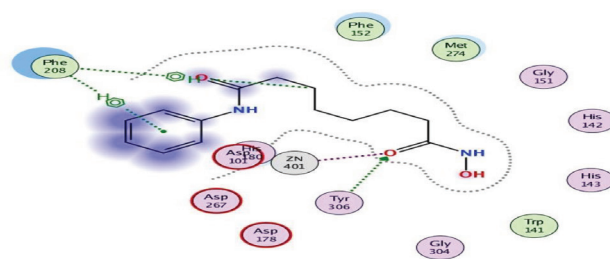


Fig. 2 Demonstration of SAHA (Vorinostat) within the binding site of HDAC-8 and the mode of interactions.

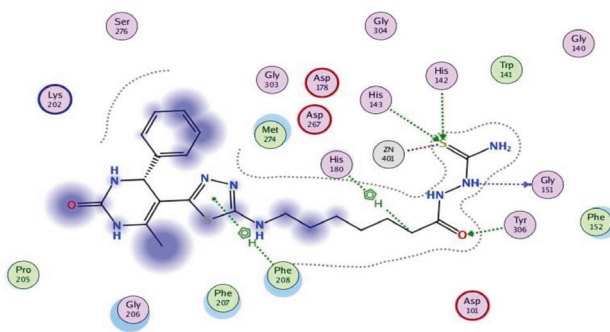


Fig. 3 Demonstration of V a,t within the binding site of HDAC-8 and the mode of interactions.

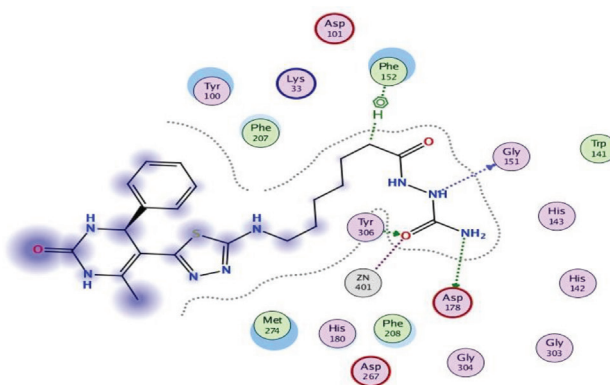


Fig. 4 Demonstration of V a,s within the binding site of HDAC-8 and the mode of interactions.

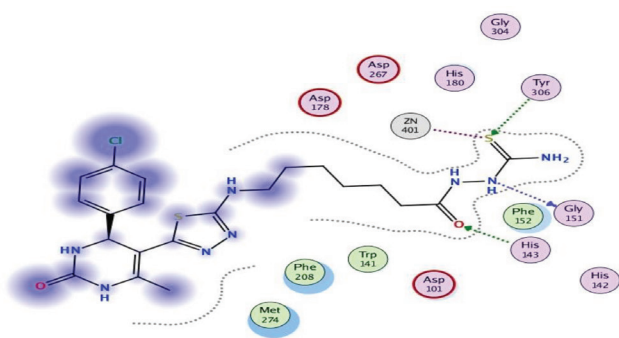


Fig. 5 Demonstration of V b,t within the binding site of HDAC-8 and the mode of interactions.

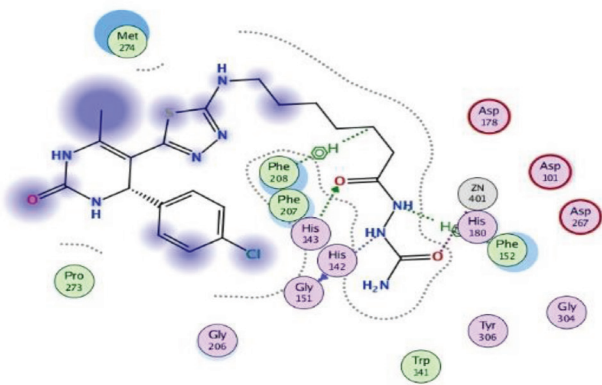


Fig. 6 Demonstration of V b,s within the binding site of HDAC-8 and the mode of interactions.

the region around  $1690\text{ cm}^{-1}$  the appearance of C=O amide bond at an area around  $1743\text{--}1674\text{ cm}^{-1}$ , and the appearance of C=O ester bond at an area around  $1701\text{--}1597\text{ cm}^{-1}$ . The  $^1\text{H-NMR}$  for compounds (I a,b), ester analogs were characterized appearance of singlet signal due to the proton at the C of CH<sub>3</sub> near 2.3 ppm, and appearance of doublet signal due to the proton at C alpha to N of heterocyclic rings near 5.4 ppm and appearance of singlet signal due to the proton of NH heterocyclic rings near 9.9 ppm.

**Compound (II a,b)** was synthesized by the reaction of ester compounds (I a,b) and sodium hydroxide (15%) at  $90^\circ\text{C}$ . The FTIR for both compounds were characterized by the disappearance of C=O band of ester in the region around  $1701\text{--}1697\text{ cm}^{-1}$ , and appearance of broad O-H band of carboxylic acid in the area around  $3400\text{--}2500\text{ cm}^{-1}$ . The  $^1\text{H-NMR}$  for compounds (II a,b), carboxylic acid analogs were characterized by the disappearance of triplet signal of proton of CH<sub>3</sub>, quartet of CH<sub>2</sub> of ethyl ester near and the appearance of singlet signal of protons of OH near 12.3 ppm.

**Compound (III a,b)** was synthesized by the reaction of thiosemicarbazide with carboxylic acid compounds (II a,b) and 70% sulfuric acid in ethanol then neutralized with concentrated ammonia. The FTIR for both compounds were characterized by disappearance O-H band of carboxylic acid in the area around  $3444\text{--}3200\text{ cm}^{-1}$  and C=O band of ester in the region around  $1701\text{--}1697\text{ cm}^{-1}$ , and appearance of an NH a primary amine band at  $3352\text{--}2966\text{ cm}^{-1}$ , C=N band in the region around  $1600\text{--}1577\text{ cm}^{-1}$  and C-S-C band at  $725\text{--}690\text{ cm}^{-1}$ . The  $^1\text{H-NMR}$  for compounds (III a,b), 1,3,4-thiadiazol-2-amino derivatives were characterized by

the disappearance of the signal of proton OH near 12.3 ppm, and appearance of proton signal of NH<sub>2</sub> at the region near 7.02 ppm.

**Compound (IV a,b)** was synthesized by the reaction of compound (III a,b), ethyl-7-bromoheptanoate and dry K<sub>2</sub>CO<sub>3</sub> in anhydrous acetone. The FTIR for both compounds were characterized by disappearance of an NH a primary amine band at  $3352\text{--}3200\text{ cm}^{-1}$ , and appearance of C=O band of ester in the region around  $1732\text{ cm}^{-1}$ , O-C band of ester at  $1157\text{--}1203\text{ cm}^{-1}$ , C-H band of (CH<sub>2</sub>)<sub>6</sub> at  $1462\text{--}1427\text{ cm}^{-1}$  and C-H band of CH<sub>2</sub>-CH<sub>3</sub> at  $1377\text{--}1373\text{ cm}^{-1}$ . The  $^1\text{H-NMR}$  for compounds (IV a,b), ester analogs characterized by the disappearance of proton signal of NH<sub>2</sub> at the region near 7.02 ppm, and apparent of NH proton as a signal at the region 7.4-7.5 ppm, several signal of CH<sub>2</sub> of the side chain, also apparent of triplet signal due to the proton at the C of CH<sub>3</sub> near 1.1 ppm.

**Compound (V a,s, V b,s, V a,t and V b,t)** was synthesized by the reaction thiosemicarbazide or semicarbazide, KOH and compound (IV a,b) using saturated Ammonium chloride aqueous solution, ethyl acetate and Sodium sulfate. The FTIR for compounds (V a,s and V b,s) were characterized by disappearance of C=O band of ester in the region around  $1732\text{ cm}^{-1}$  and the appearance of C=O amide band at  $1604\text{--}1597\text{ cm}^{-1}$ , an NH a primary amine band at  $3309\text{--}3032\text{ cm}^{-1}$ . The  $^1\text{H-NMR}$  for compounds (V a,s and V b,s), were characterized by disappearance of proton signal of NH<sub>2</sub> at the region near 7.02 ppm, and apparent of NH proton as a signal at the region 7.4-7.5 ppm, several signal of CH<sub>2</sub> of the side chain, also apparent of triplet signal due to the proton at the C of CH<sub>3</sub> near 1.1 ppm. The FTIR for compounds (V a,t and V b,t) were characterized by disappearance of C=O band of ester in the region around  $1732\text{ cm}^{-1}$  and the appearance of C=O amide band at  $1604\text{--}1597\text{ cm}^{-1}$ , an NH a primary amine band at  $3309\text{--}3221\text{ cm}^{-1}$ , C=S band at  $1261, 1253\text{ cm}^{-1}$ . The  $^1\text{H-NMR}$  for compounds (V a,t and V b,t), were characterized by disappearance of triplet signal due to the proton at the C of CH<sub>3</sub> near 1.1 ppm, and apparent of proton signal of NH<sub>2</sub> at the region near 6.4-7.2 ppm.

### In Vitro Cytotoxicity Assay

The anticancer activity of compound (V a,s, V b,s, V a,t, and V b,t) were examined in the dose-response curve generated by Prism Pad 8.1 using nonlinear regression analysis for compounds in MCF-7 cells and HRT-18 cells is shown below figures. The IC<sub>50</sub> values were obtained to a range of concentrations of compounds from (100 – 1.56  $\mu\text{M}$ ) by MTT assay. See Figures 7–11.

#### a) Cytotoxicity of compounds against human colon adenocarcinoma (HRT-18):

IC<sub>50</sub> of V a,t in human colon adenocarcinoma (HRT-18) = 69.48  $\mu\text{M}$

IC<sub>50</sub> of V b,t in human colon adenocarcinoma (HRT-18) = 71.81  $\mu\text{M}$

#### b) Cytotoxicity of compounds against Breast cancer cell line (MCF7):

IC<sub>50</sub> of V a,t in Breast Cancer Cell Line (MCF-7) = 0.69  $\mu\text{M}$

IC<sub>50</sub> of V b,t in Breast Cancer Cell Line (MCF-7) = 0.75  $\mu\text{M}$

### Discussion

According to the above-mentioned results, the synthetic compounds (V a,s and V b,s) does not show any cytotoxicity against the two cell line while (V a,t, V b,t,) are useful for the

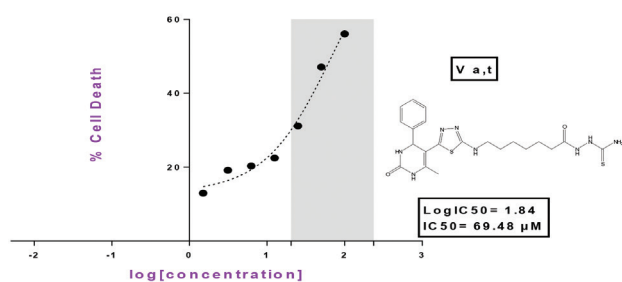


Fig. 7 Dose-response curves of IC<sub>50</sub> for V a,t. HRT-18 cells were treated for 72hr. with 0.05, 0.15, 0.32, 0.75, 1.56, 3.12, 6.25, 12.5, 25, 50 and 100 μM dose ranges of V a,t. The dose response for V a,t was plotted over log transformed V a,t concentrations. IC<sub>50</sub> values were determined using nonlinear regression analysis (Prism Pad 8.1). Results represent for triplicate data.

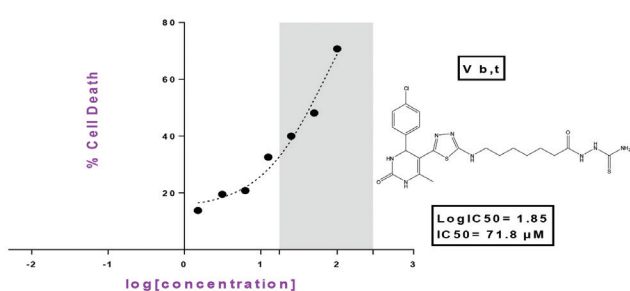


Fig. 8 Dose-response curves of IC<sub>50</sub> for V b,t. HRT-18 cells were treated for 72hr. with 0.05, 0.15, 0.32, 0.75, 1.56, 3.12, 6.25, 12.5, 25, 50 and 100 μM dose ranges of V b,t. The dose response for V b,t was plotted over log transformed V b,t concentrations. IC<sub>50</sub> values were determined using nonlinear regression analysis (Prism Pad 8.1). Results represent for triplicate data.

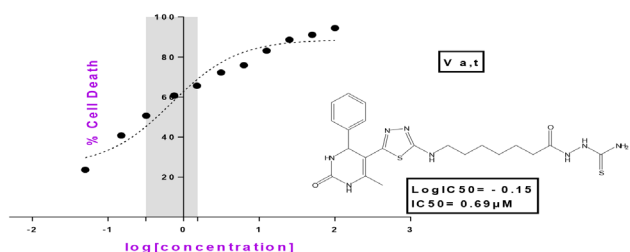


Fig. 9 Dose-response curves of IC<sub>50</sub> for V a,t. MCF-7 cells were treated for 72hr. with 0.05, 0.15, 0.32, 0.75, 1.56, 3.12, 6.25, 12.5, 25, 50 and 100 μM dose ranges of V a,t. The dose response for V a,t was plotted over log transformed V a,t concentrations. IC<sub>50</sub> values were determined using nonlinear regression analysis (Prism Pad 8.1). Results represent for triplicate data.

treatment of breast cancer and human colon adenocarcinoma, as they inhibit the HDAC enzyme through the presence of common pharmacophores consisting of three distinct domains as shown below:

- (1) A surface recognition unit or cap group which usually a hydrophobic and aromatic group or may be heteroaromatic,<sup>27</sup> which interacts with the rim of the binding pocket. The cap group could be linked to the aliphatic linker group through either hydrogen-bond accepting or donating groups such as keto- and amide-groups.

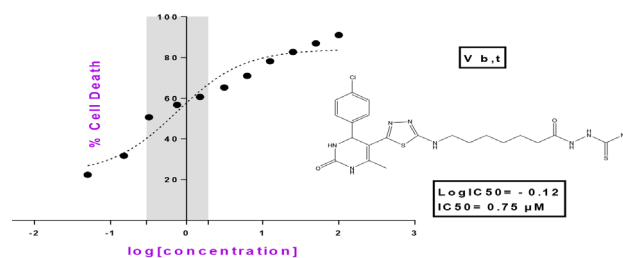


Fig. 10 Dose-response curves of IC<sub>50</sub> for V b,t. MCF-7 cells were treated for 72hr. with 0.05, 0.15, 0.32, 0.75, 1.56, 3.12, 6.25, 12.5, 25, 50 and 100 μM dose ranges of V b,t. The dose response for V b,t was plotted over log transformed V b,t concentrations. IC<sub>50</sub> values were determined using nonlinear regression analysis (Prism Pad 8.1). Results represent for triplicate data.

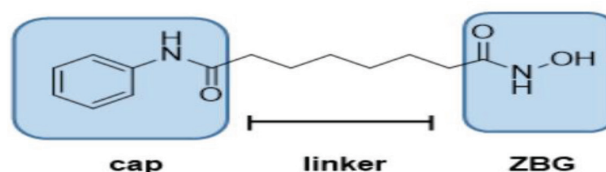


Fig. 11 Structure of SAHA.

- (2) A zinc binding group (ZBG) or zinc binding domain (ZBD), such as the hydroxamic acid, benzamide, carboxylic acid, amide or biguanide groups,<sup>28,29</sup> which coordinates with of Zn<sup>2+</sup> ion in the active site outer surface.
- (3) A linker domain that is either saturated or unsaturated with linear or cyclic structure, connects the cap group to the ZBD.<sup>30</sup> These are best illustrated by the classical, FDA-approved inhibitor suberoylanilide hydroxamic acid (SAHA).

## Conclusion

In the recent decade, there have been several drugs to treat breast and colon cancer. However, there is still an unmet need to develop different types of drugs to reduce systemic toxicity and improve therapeutic efficacy. In the present study, we synthesized three compounds (V a,t, V b,t). The chemical structures of the synthesized compounds were confirmed by FT-IR and <sup>1</sup>H-NMR. MTT assay demonstrated *In vitro* cytotoxicity study against MCF-7 and HRT-18, for compounds (V a,t, and V b,t) show a good inhibition ratio to this cell line compared to SAHA. Therefore, these newly synthesized analogs may be represented as an exploitable source of new anticancer agents fighting breast cancer.

## Conflict of Interest

The authors have no conflicts of interest regarding this investigation.

## Acknowledgments

We thank the Department of Pharmaceutical Chemistry/College of the Pharmacy/University of Baghdad for their official support in this study. ■

## References

1. Baretti M, Azad NS. The role of epigenetic therapies in colorectal cancer. *Current Problems in Cancer*. 2018;42(6):530-47.
2. Baylin SB, Jones PA. Epigenetic determinants of cancer. *Cold Spring Harbor Perspectives in Biology*. 2016;8(9):a019505.
3. Bunkar N, Pathak N, Lohiya NK, Mishra PK. Epigenetics: A key paradigm in reproductive health. *Clinical and Experimental Reproductive Medicine*. 2016;43(2):59.
4. Sharma S, Kelly TK, Jones PA. Epigenetics in cancer. *Carcinogenesis*. 2010;31(1):27-36.
5. Manal M, Manish K, Sanal D, Selvaraj A, Devadasan V, Chandrasekar M. Novel HDAC8 inhibitors: A multi-computational approach. *SAR and QSAR in Environmental Research*. 2017;28(9):707-33.
6. Parbin S, Kar S, Shilpi A, Sengupta D, Deb M, Rath SK, et al. Histone deacetylases: a saga of perturbed acetylation homeostasis in cancer. *Journal of Histochemistry & Cytochemistry*. 2014;62(1):11-33.
7. Ruijter AJd, GENNIP AHv, Caron HN, Kemp S, KUILENBURG ABv. Histone deacetylases (HDACs): characterization of the classical HDAC family. *Biochemical Journal*. 2003;370(3):737-49.
8. Zhou H, Wang C, Ye J, Chen H, Tao R. Design, virtual screening, molecular docking and molecular dynamics studies of novel urushiol derivatives as potential HDAC2 selective inhibitors. *Gene*. 2017; 637:63-71.
9. Eckschlager T, Plch J, Stiborova M, Hrabeta J. Histone deacetylase inhibitors as anticancer drugs. *International Journal of Molecular Sciences*. 2017;18(7):1414.
10. Zwick V, Chatzivasileiou A-O, Deschamps N, Roussaki M, Simões-Pires CA, Nurisso A, et al. Aurones as histone deacetylase inhibitors: Identification of key features. *Bioorganic & Medicinal Chemistry Letters*. 2014;24(23): 5497-501.
11. Cappellacci L, Perinelli DR, Maggi F, Grifantini M, Petrelli R. Recent progress in histone deacetylase inhibitors as anticancer agents. *Current Medicinal Chemistry*. 2020;27(15):2449-93.
12. Yoon S, Kang G, Eom GH. HDAC inhibitors: therapeutic potential in fibrosis-associated human diseases. *International Journal of Molecular Sciences*. 2019;20(6):1329.
13. Yu C, He F, Qu Y, Zhang Q, Lv J, Zhang X, et al. Structure optimization and preliminary bioactivity evaluation of N-hydroxybenzamide-based HDAC inhibitors with Y-shaped cap. *Bioorganic & Medicinal Chemistry*. 2018;26(8):1859-68.
14. Brindisi M, Senger J, Cavella C, Grillo A, Chemi G, Gemma S, et al. Novel spiroindoline HDAC inhibitors: Synthesis, molecular modelling and biological studies. *European Journal of Medicinal Chemistry*. 2018; 157:127-38.
15. Liu R, Wang J, Tang W, Fang H. Design and synthesis of a new generation of substituted purine hydroxamate analogs as histone deacetylase inhibitors. *Bioorganic & Medicinal Chemistry*. 2016;24(7):1446-54.
16. Manal M, Chandrasekar M, Priya JG, Nanjan M. Inhibitors of histone deacetylase as antitumor agents: A critical review. *Bioorganic Chemistry*. 2016; 67:18-42.
17. Huang M, Zhang J, Yan C, Li X, Zhang J, Ling R. Small molecule HDAC inhibitors: Promising agents for breast cancer treatment. *Bioorganic Chemistry*. 2019; 91:103184.
18. Ding J, Liu J, Zhang Z, Guo J, Cheng M, Wan Y, et al. Design, synthesis and biological evaluation of coumarin-based N-hydroxycinnamamide derivatives as novel histone deacetylase inhibitors with anticancer activities. *Bioorganic Chemistry*. 2020; 101:104023.
19. Berman HM, Westbrook J, Feng Z, Gilliland G, Bhat TN, Weissig H, et al. The protein data bank. *Nucleic Acids Research*. 2000;28(1):235-42.
20. Saloutin V, Burgart YV, Kuzueva O, Kappe C, Chupakhin O. Biginelli condensations of fluorinated 3-oxo esters and 1, 3-diketones. *Journal of Fluorine Chemistry*. 2000;103(1):17-23.
21. K Hameed K, HS Hussain F. Ultrasound-Assisted Synthesis of Some New N-(Substituted Carboxylic Acid-2-yl)-6-Methyl-4-Substituted Phenyl-3, 4-Dihydropyrimidine-2 (1H)-One Carboxamides. *Eurasian Journal of Science and Engineering*. 2018;4(2).
22. Barbosa G, de Aguiar A. Synthesis of 1, 3, 4-Thiadiazole Derivatives and Microbiological Activities: A Review. *Revista Virtual de Química*. 2019;11(3):806-48.
23. González-Martínez D, Fernández-Sáez N, Catiuela C, Campos JM, Gotor-Fernández V. Development of Biotransamination Reactions towards the 3, 4-Dihydro-2 H-1, 5-benzoxathiepin-3-amine Enantiomers. *Catalysts*. 2018;8(10):470.
24. Yang F, Zhao N, Song J, Zhu K, Jiang C-s, Shan P, et al. Design, synthesis and biological evaluation of novel coumarin-based hydroxamate derivatives as histone deacetylase (hdac) inhibitors with antitumor activities. *Molecules*. 2019;24(14):2569.
25. Deyrieux AF, Wilson VG. In vitro culture conditions to study keratinocyte differentiation using the HaCaT cell line. *Cytotechnology*. 2007;54(2):77-83.
26. Riss TL, Moravec RA, Niles AL, Duellman S, Benink HA, Worzella TJ, et al. *Cell Viability Assays*. Assay Guid Man [Internet]. 2016;1-25. Available from: <http://www.ncbi.nlm.nih.gov/pubmed/23805433>.
27. Sarah S. Jabbar, Mohammed H. Mohammed. Coumarin based-histone deacetylase HDAC inhibitors. *Egyptian Journal of Chemistry*. 2022;65(7)379-384.
28. Duraid Al-Amily, Mohammed H. Mohammed. Design, Synthesis and Cytotoxicity Study of Primary Amides as Histone Deacetylase Inhibitors. *Iraqi J Pharm Sci*. 2019.Vol.28(2) .
29. Othman M. Sagheer, Mohammed H. Mohammed, Jaafar S. Wadi, and Zaid O. Ibraheem. Studying the Cytotoxic Activity of Newly Designed and Synthesized HDAC 2100346.
30. Miller TA, Witter DJ, Belvedere S. Histone deacetylase inhibitors. *Journal of Medicinal Chemistry*. 2003;46(24):5097-116.

This work is licensed under a Creative Commons Attribution-NonCommercial 3.0 Unported License which allows users to read, copy, distribute and make derivative works for non-commercial purposes from the material, as long as the author of the original work is cited properly.